Advanced Solidification Processing of an Industrial Gas Turbine Engine Component

Mei Ling Clemens, Allen Price, and Richard S. Bellows

This paper will describe the efforts of the Advanced Turbine Airfoil Manufacturing Technology Program sponsored by the U.S. Department of Energy through the Oak Ridge National Laboratory and Howmet Research Corporation. The purpose of the program is to develop single-crystal and directionally solidified casting technologies to benefit Advanced Turbine Systems (ATS) industrial and utility gas turbine engines. The focus is on defining and implementing advanced Vacuum Induction Melting (VIM) furnace enhancements that provide precise control of mold temperatures during solidification. Emphasis was placed on increasing the total magnitude of thermal gradients while minimizing the difference in maximum and minimum gradients produced during the solidification process. Advanced VIM casting techniques were applied to Solar Turbines Incorporated's Titan 130 First Stage High Pressure Turbine Blade under the ATS program. A comparison of the advanced VIM casting process to the conventional Bridgeman casting process will be presented as it pertains to the thermal gradients achieved during solidification, microstructure, elemental partitioning characterization, and solution heat treat response.

INTRODUCTION

For the past 30 years, the casting of single-crystal aerospace turbine blades has been optimized to the point that yields greater than 95% are commonly achieved. Although this work has provided an in-depth understanding of the relationships of alloy, geometry, and process conditions, the application of this knowledge to industrial and utility gas turbine blades has proven to be challenging at best. The physical size of these components has pushed this technology to the point that additional advances in investment casting are in order. The need for higher thermal gradients and solidification rates by the superalloy community has led to some shifts in the processing paradigm. The development of casting technologies such as liquid metal cooling and gas-assisted cooling has resulted in improvements in this area. These technologies, however, require significant development prior to incorporating them into production.

To further this effort, the U.S. Department of Energy, through the Oak Ridge National Laboratory and Howmet Research Corporation, established the Advanced Turbine Airfoil Manufacturing Technology Program. The purpose of the program was to develop single-crystal and directionally solidified casting technologies to benefit advanced-turbine systems (ATS) industrial and utility gas-turbine casting components. The focus of the program was to define and implement advanced vacuum-induction melting (VIM) furnace and control enhancements that would provide precise control of mold temperatures during solidification. Consequently, the enhancements would improve thermal gradients and solidification rates of these larger components.

Finer dendritic arm spacing, reduced elemental segregation, and reduced grain defects are typical expectations of a higher thermal gradient/solidification rate casting process. These microstructural refinements can also assist in the reduction of solution heat treatment cycles as improved homogenization behavior can be realized. Additional benefits are expected from this program as these enhancement features can be readily implemented into existing Bridgeman-style casting furnaces, thus significantly reducing the time to implementation.

TECHNICAL APPROACH

Two casting processes were conducted during the evaluation—the conventional Bridgeman process and a high-gradient Bridgeman process. The conventional Bridgeman process is utilized in today's production of investment casting of single-crystal turbine blades. The high-gradient process is the product of furnace and control enhancements applied to a Bridgeman furnace.

The Solar Titan 130 High Pressure First Stage Turbine blade, as shown in Figure 1, was selected as the casting configuration for this study. The Titan 130 first-stage blade is a single-crystal casting with complex internal cooling passages. As a production blade, casting defects such as high-angle grain boundaries, recrystallized grains, and freckles, are occasionally encountered.

Figure 1. The Solar Turbines Titan™ 130 first high pressure turbine blade utilized in this casting evaluation.

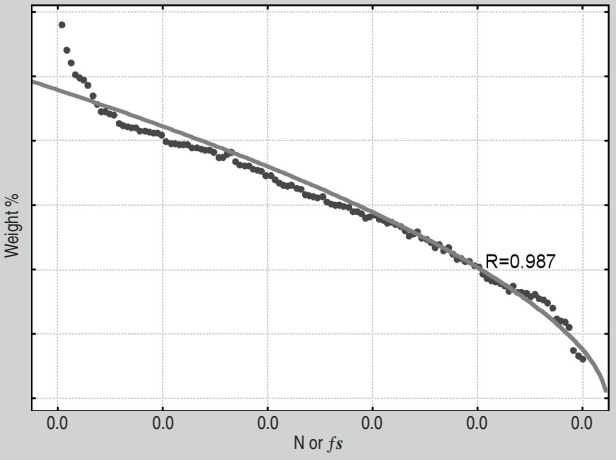

Figure 2. The elemental data ranked in descending order and plotted as a function of normalized order. The Scheil-Gulliver equation is fitted to the ordered data.

Ceramic molds comprising turbine blades and mechanical test specimens were cast at Howmet Research Corporation in Whitehall, Michigan. Each mold was instrumented with thermocouples in order to evaluate the temperatures and resulting thermal gradients achieved. All castings were solution heat treated at Howmet's production facility.

Microstructural evaluations were conducted on the airfoil and root areas of the turbine blade. This was done to represent the thinnest and thickest cross-sections of the part configuration. Both casting processes were evaluated in the as-cast and solution-heat-treated condition. Primary and secondary dendritic arm spacing measurements, maximum segregation, elemental partitioning analysis, and crystal orientation were also examined.

The maximum segregation was calculated using the delta between the maximum and minimum elemental weight percent measured from the microprobe data that was utilized for the partitioning analysis.

Partitioning Analysis

Elemental partitioning analysis was utilized to study the resulting segregation produced by the casting process and its impact on homogenization after solution heat treatment. A statistically significant point count methodology was employed to obtain elemental partition information.[1–4] Electron-microprobe data was collected in a 121-point square grid measuring 1,000 μm wide. Dendritic and interdendritic areas were included in the measurements while carbides and casting porosity were avoided in the analysis.

The elemental data collected was then ranked in descending or ascending order based upon where the element partitioned to (i.e., dendritic or interdendritic regions). Elements such as Ni, Al, Ta, Ti, and Hf ranked in ascending order partition to the interdendritic regions. Elements partitioning to the dendritic areas, such as Cr, Re, Co, W, and Mo, were ranked in descending order. A visual representation of this data is made by plotting this ranked elemental data in weight percent as a function of ranking order normalized to 1 (denoted as N or f_s) and is illustrated in Figure 2.

The elemental partition coefficient, k, was derived from the ranked data by the Scheil-Gulliver Equation 1 and was equated to the slope of the curve as illustrated in Figure 2.

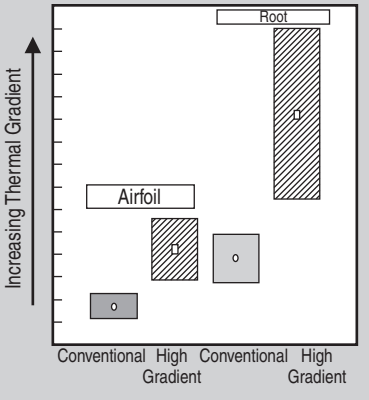

Figure 3. The average, maximum, and minimum thermal gradients achieved for the conventional and high-gradient processes compared in this study.

$$C_l = C_o(1-(1-2\alpha k)f_s)^{\frac{k-1}{1-2\alpha k}} \quad (1)$$

Here C_l is the concentration in the liquid, C_o is the nominal composition, α is the Fourier number, and f_s is the fraction solid (equivalent to the normalized ranked order).

Partitioning values equivalent to 1 indicate that an element is homogeneously distributed between the interdendritic and dendritic regions. k values less than 1 indicate elements partitioning to the liquid during solidification. Elements with k values less than 1 typically have higher concentrations in the interdendritic eutectic regions in the completely solidified microstructure. Conversely, k values greater than 1 result in elements partitioning to the solid and with higher elemental concentration in the dendritic regions. Consequently, the success criteria of this analysis is to achieve partitioning values closest to the value of 1. This will indicate less segregation, should have the smallest difference between the maximum and minimum elemental composition measured, and is visually illustrated on a ranked plot by a flat curve. Through solution heat treatment, additional partitional analysis will result in k values closer to 1 when compared to the as-cast k values.

RESULTS AND DISCUSSION

Thermal Gradients and Mushy Zone Size

Using the high-gradient casting process, thermal gradient improvements of 60% were obtained in the airfoil and 90% in the root section. Shown in Figure 3, the plot for the average, maximum, and minimum gradients for both processes illustrates that a higher gradient is achieved with the improved casting process. Inherent to the high-gradient process, a larger spread between the maximum and minimum gradient in the root was produced. However, the high-gradient process decreased the mushy zone size along the solidification direction by 29% for the airfoil and 41% for the root.

Microstructural Improvements

The improvements in primary and secondary dendritic arm spacing mea-

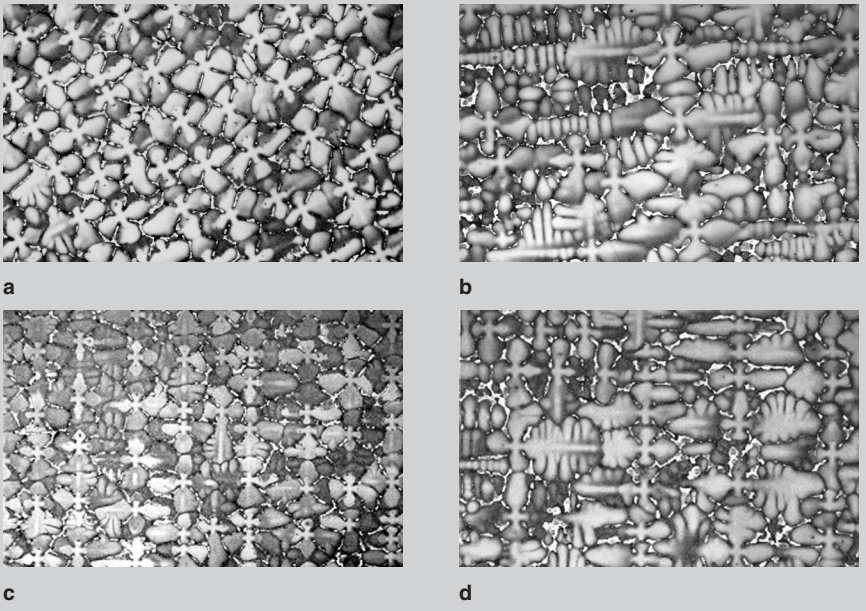

Figure 4. Optical micrographs of the as-cast microstructures produced using the conventional casting in (a) the airfoil section and (b) the root section and using high-gradient casting in (c) the airfoil section and (d) the root section.

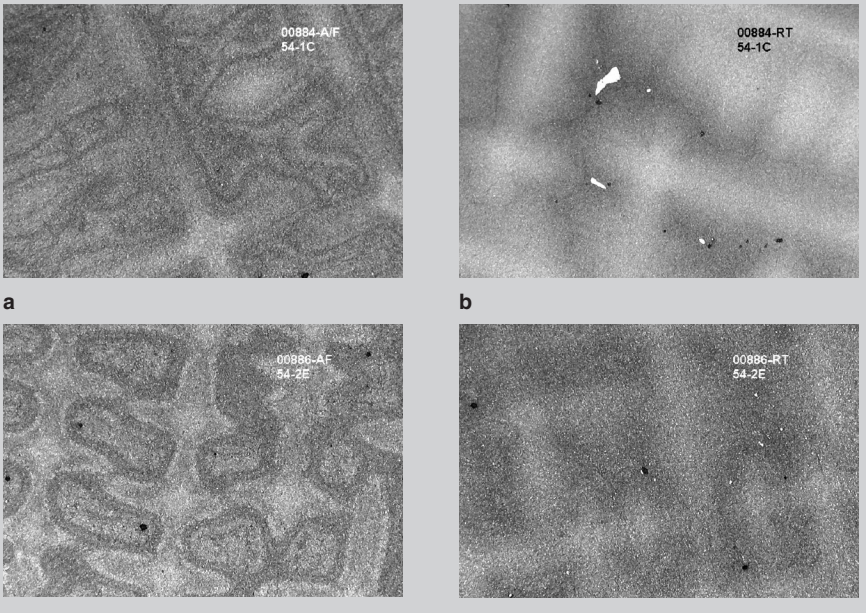

Figure 5. Optical micrographs of the solutioned microstructures produced using the conventional casting in (a) the airfoil section and (b) the root section and using high-gradient casting in (c) the airfoil section and (d) the root section.

surements are presented in Table I. For primary dendritic arm spacing measurements, a 13% improvement was achieved in the airfoil section while a 26% improvement was achieved in the root section. Secondary dendritic arm spacing measurements obtained a 9% improvement regardless of cross-sectional thickness. Optical micrographs showing the resulting as-cast microstructures are presented in Figure 4.

The interdendritic eutectic levels varied with the casting process and are presented in Table II. Lower levels were observed in the root section of the high-gradient process. They were equivalent and higher for both processes in the airfoil sections.

Solution heat treatment produced solutioning levels greater than 99% for both casting processes. Conventional and high-gradient microstructures

Table I. Improvements over the Standard Bridgeman Process for the Titan 1st Blade

	Airfoil	Root
Primary dendritic arm spacing	13%	26%
Secondary dendritic arm spacing	9%	9%

Table II. As-Cast Interdendritic Eutectic Measured for the Bridgeman Processes

	Conventional	High-Gradient
Root	24.9%	20.2%
Airfoil	27.3%	27.0%

are presented in Figure 5. Typical casting porosity was observed and was comparable for both casting processes.

Maximum Segregation and Partitioning Results

All maximum segregation and calculated partitioning values are summarized in Tables III and IV. Graphs of the maximum segregation for the airfoil and root are presented in Figure 6. As-cast and solutioned conditions are presented in this figure. The as-cast elemental segregation was measured to be within 1 wt.% for both casting processes in the airfoil and root sections. However, the partitioning of elements during solidification was not comparable nor consistently higher or lower within a single casting process, as can be seen in Figure 7.

Elements such as Ni, Co, and Al had comparable partitioning from airfoil to root and for both casting processes. For the remainder of the elements, partitioning was influenced more by the cross-sectional differences and gradient processes. Within a given cross-sectional thickness, k values for Cr, Mo, Re, and W were higher for the high-gradient process. Partitioning was also shown to increase with a thicker cross-section.

The higher segregation observed in the as-cast condition is attributed to the finer dendritic microstructure producing higher concentration gradients.[5] This resulted in improved solutioning behavior being consistently observed from the blades produced by the high-gradient casting process. The solution-

Table III. Maximum Segregation Measured in the Conventional and High-Gradient Process for As-Cast and Solution Heat Treated Turbine Blades

	Ni	Co	Ti	Al	Ta	Cr	Mo	Re	W
Airfoil									
Conventional process As-cast condition	14.18	5.09	1.55	3.23	8.93	7.76	0.71	5.19	7.57
High-gradient process As-cast condition	11.35	4.29	1.76	3.29	8.67	6.98	0.76	5.72	8.11
Conventional process Solutioned heat treated	4.09	1.20	0.15	1.08	1.46	1.56	0.25	1.64	1.72
High-gradient process Solutioned heat treated	2.83	0.48	0.12	0.62	1.04	0.93	0.25	1.41	1.53
Root									
Conventional process As-cast condition	8.39	3.54	1.67	2.68	7.85	8.02	0.80	4.43	7.35
High-gradient process As-cast condition	12.10	3.81	1.63	2.71	8.01	8.49	0.85	4.60	7.62
Conventional process Solutioned heat treated	4.60	1.84	0.23	1.46	2.03	1.86	0.31	2.50	2.43
High-gradient process Solutioned heat treated	2.83	0.93	0.12	0.62	0.72	0.48	0.25	1.41	1.53

Table IV. Partitioning Ratios for the Conventional and High-Gradient Bridgeman Casting Processes in the As-Cast and Solutioned Conditions

	Ni	Co	Ti	Al	Ta	Cr	Mo	Re	W
As-Cast									
Conventional airfoil	0.96	1.11	0.73	0.87	0.78	1.19	1.31	1.57	1.34
High-gradient airfoil	0.96	1.13	0.69	0.86	0.72	1.27	1.36	1.81	1.45
Conventional root	0.96	1.11	0.65	0.87	0.72	1.21	1.3	1.7	1.47
High-gradient root	0.95	1.11	0.69	0.87	0.73	1.25	1.44	1.9	1.53
Solutioned Heat Treated									
Conventional airfoil	0.98	1.03	0.97	0.96	0.96	1.05	1.12	1.28	1.07
High-gradient airfoil	0.99	1.02	0.98	0.97	0.97	1.02	1.09	1.15	1.07
Conventional root	0.98	1.05	0.94	0.94	0.92	1.09	1.15	1.26	1.11
High-gradient root	0.98	1.02	0.97	0.97	0.97	1.02	1.1	1.15	1.07

ing behavior was notably improved using the high-gradient process as the maximum segregation in the root section decreased by more than 1 wt.%, as shown in Figure 6.

This was substantiated by the k values presented in Figure 8, as all k values for the high-gradient process were closer to 1. The expectations of a high-gradient process are that decreased segregation and improved partitioning behavior are typically produced. For the gradient conditions obtained in this study, the typical results were not observed. Since a lower thermal gradient and a larger mushy zone were produced by the conventional process, back diffusion of the elements may have contributed to the lower segregation and partitioning obtained.

The finer microstructure obtained via a smaller primary dendritic arm spacing for the high-gradient process contributed to the improved solutioning behavior. This finer microstructure provided smaller diffusion distances for elemental solutioning. This is particularly important for heavy and slow diffusing elements such as Re, W, and Ta.

Crystal Orientation and Grain Defects

Stereographic orientation triangles showing the resulting Laue results are presented in Figure 9 for the mechanical test bars and turbine blades. The crystal orientation of the mechanical test bars were noted to be considerably better for the high-gradient process. The impact of thermal gradients and part configuration on crystal orientation can be clearly seen in Figure 9 when comparing the orientation maps of the mechanical test bars to the turbine blades. As the test bars are cylindrical in shape and do not contain the complex features of a turbine blade, the test bars contain a closer <001> crystal orientation than the blades with the high-gradient casting process.

Casting configurations have been known to influence thermal gradients by impacting the shape and location of the solidification front as it progresses through varying cross-sectional thickness within a part.[5–10] This, in turn, will influence the resulting crystal orientation. Curved solidification fronts typically contain higher horizontal thermal gradient components (i.e., perpendicular to the solidification direction) and lower vertical thermal gradient components (i.e., parallel to the solidification direction). Deviations from the vertical thermal gradient component will cause the developing dendritic tip to splay away from the desired growth orientation.

Casting features, such as platforms, are more susceptible to grain defects if these horizontal components are significant enough to nucleate a new grain. This indicates that the casting configuration and geometrical arrangement on the mold must be carefully considered in addition to the high-gradient process itself. This was substantiated through examination of the grain defects produced in this study and is reported in Table V.

Fifty percent of all defects formed in

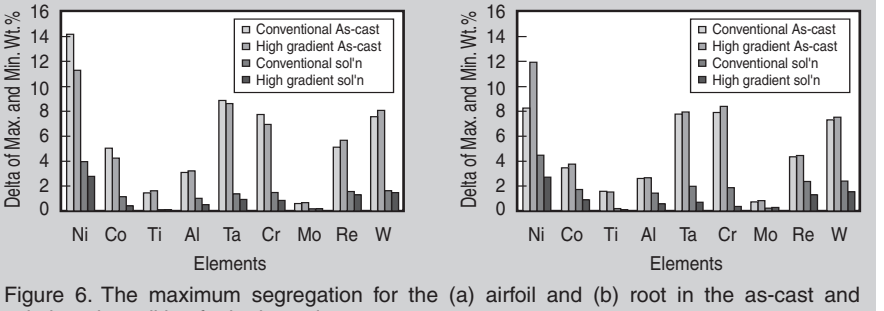

Figure 6. The maximum segregation for the (a) airfoil and (b) root in the as-cast and solutioned condition for both casting processes.

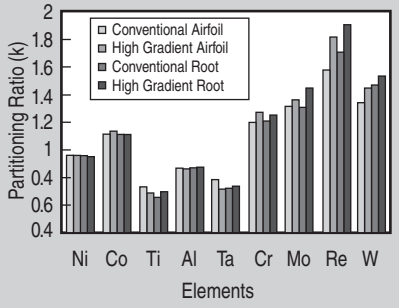

Figure 7. The calculated partitioning ratios for conventional and high-gradient castings in the as-cast condition. A partitioning ratio approaching 1 indicates equivalent partitioning between the interdendritic and dendritic regions.

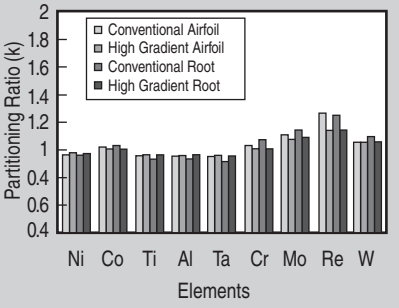

Figure 8. The calculated partitioning ratios for conventional and high-gradient castings in the solution heat-treated condition. A partitioning ratio approaching 1 indicates equivalent partitioning between the interdendritic and dendritic regions.

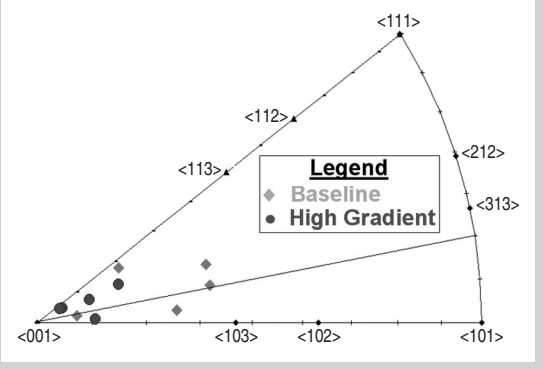

a

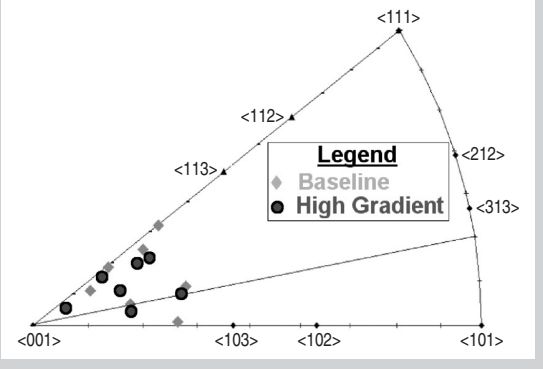

b

Figure 9. Stereographic orientation maps showing Laue results for (a) mechanical test bars and (b) turbine blades cast using the conventional (baseline) and high-gradient process.

Table V. Number of Grain Defects Observed on the Titan 130 1st Blade Cast Using Conventional and High-Gradient Processes

	Conventional	High-Gradient	Location
Freckle chains	4	1	Root
High angle boundaries	3	2	Leading-edge platform, trailing edge, root
Recrystallized grains	1	4	Concave platform edge, leading edge
Zebra grains	0	1	Leading-edge platforms

the conventional process were due to freckle formation in the root area. High angle boundaries were also numerous and comprised 37% of the remainder of the defects. The high-gradient process reduced the number of freckles but the occurrence of high angle boundaries and recrystallized grains increased. The platform and root areas were primary locations for these defects. Recrystallized and zebra grains constituted 63% of all defects observed in the high-gradient process. As these grain defects occurred in the platform area (i.e., where a thin cross-sectional area meets up with a thick cross-sectional area [root]), thermal stresses between the shell and casting can impart residual stresses as a consequence to the steeper thermal gradient. These high residual stress areas would become a source for recrystallization during solution heat treatment. Close attention to such geometrical aspects are imperative if the high-gradient process is to be successful in a production environment.

References

1. M.N. Gungor, "A Statistically Significant Experimental Technique for Investigating Microsegregation in Cast Alloys," *Metall. Trans. A,* 20A (1989), p. 2529.
2. N. D'Souza, B.A. Shollock, and M. McLean, "Quantitative Characterisation of Microsegregation and Competitive Grain Growth in CMSX-4," *Solidification Processing 1997,* ed. J. Beech and H. Johnes (Sheffield, U.K.: Department of Engineering Materials, 1997), pp. 316–342.
3. M.S.A. Karunaratne et al., "Modelling of the Microsegregation in CMSX-4 Superalloy and its Homogenisation during Heat Treatment," *Superalloys 2000,* ed. T.M. Pollock, R.D. Kissinger, and R.R. Bowman (Warrendale, PA: TMS, 2000), p. 263.
4. S. Tin, T.M. Pollock, and W.T. King, "Carbon Additions and Grain Defect Formation in High Refractory Nickel-Base Single Crystal Superalloys," in Ref. 3, pp. 201–210.
5. A. Lohmüller et al., "Improved Quality and Economics of Investment Castings by Liquid Metal Cooling—The Selection of Cooling Media," in Ref. 3, pp. 181–188.
6. M. Konter, E. Kats, and N. Hofmann, "A Novel Casting Process for Single Crystal Gas Turbine Components," in Ref. 3, pp. 189–200.
7. S.U. An et al., "The Thermal Analysis of the Mushy Zone and Grain Structure Changes During Directional Solidification of Superalloys," in Ref. 3, pp. 247–254.
8. M.G. Ardakami et al., "Competitive Grain Growth and Texture Evolution during Solidification of Superalloys," in Ref. 3, pp. 219–228.
9. M. Eric Schlienger, "Closed Loop Control Techniques for the Growth of Single Crystal Turbine Components," *Superalloys 1996* (Warrendale, PA: TMS, 1996), pp. 487–495.
10. I.A. Wagner and P.R. Sahm, "Autonomous Directional Solidification (ADS), A Novel Casting Technique for Single Crystal Components," *Superalloys 1996* (Warrendale, PA: TMS, 1996), pp. 487–506.

Mei Ling Clemens and Allen Price are with Howmet Research Corporation. Richard S. Bellows is with Solar Turbines.

For more information, contact Mei Ling Clemens, Howmet Research Corporation, 1500 S. Warner Street, Whitehall, MI 49461; (231) 894-7055; e-mail mclemens@howmet.com.